Clinical Infectious Diseases

MAJOR ARTICLE

Comparative Replication and Immune Activation Profiles of SARS-CoV-2 and SARS-CoV in Human Lungs: An Ex Vivo Study With Implications for the Pathogenesis of COVID-19

Hin Chu,[1,a] Jasper Fuk-Woo Chan,[1,2,3,4,a] Yixin Wang,[1,a] Terrence Tsz-Tai Yuen,[1,a] Yue Chai,[1] Yuxin Hou,[1] Huiping Shuai,[1] Dong Yang,[1] Bingjie Hu,[1] Xiner Huang,[1] Xi Zhang,[1] Jian-Piao Cai,[1] Jie Zhou,[1] Shuofeng Yuan,[1] Kin-Hang Kok,[1] Kelvin Kai-Wang To,[1,2,3] Ivy Hau-Yee Chan,[5] Anna Jinxia Zhang,[1] Ko-Yung Sit,[5] Wing-Kuk Au,[5] and Kwok-Yung Yuen[1,2,3,4]

[1]State Key Laboratory of Emerging Infectious Diseases, Carol Yu Centre for Infection, Department of Microbiology, Li Ka Shing Faculty of Medicine, The University of Hong Kong, Pokfulam, Hong Kong Special Administrative Region, China, [2]Department of Microbiology, Queen Mary Hospital, Pokfulam, Hong Kong Special Administrative Region, China, [3]Department of Clinical Microbiology and Infection Control, The University of Hong Kong–Shenzhen Hospital, Shenzhen, China, [4]Hainan Medical University–The University of Hong Kong Joint Laboratory of Tropical Infectious Diseases, Hainan Medical University, Haikou, Hainan, and The University of Hong Kong, Pokfulam, Hong Kong Special Administrative Region, China, and [5]Department of Surgery, The University of Hong Kong, Queen Mary Hospital, Pokfulam, Hong Kong Special Administrative Region, China

(See the Editorial Commentary by O'Brien et al on pages 1410–2.)

Background. Severe acute respiratory syndrome coronavirus 2 (SARS-CoV-2) is an emerging coronavirus that has resulted in more than 2 000 000 laboratory-confirmed cases including over 145 000 deaths. Although SARS-CoV-2 and SARS-CoV share a number of common clinical manifestations, SARS-CoV-2 appears to be highly efficient in person-to-person transmission and frequently causes asymptomatic or presymptomatic infections. However, the underlying mechanisms that confer these viral characteristics of high transmissibility and asymptomatic infection remain incompletely understood.

Methods. We comprehensively investigated the replication, cell tropism, and immune activation profile of SARS-CoV-2 infection in human lung tissues with SARS-CoV included as a comparison.

Results. SARS-CoV-2 infected and replicated in human lung tissues more efficiently than SARS-CoV. Within the 48-hour interval, SARS-CoV-2 generated 3.20-fold more infectious virus particles than did SARS-CoV from the infected lung tissues ($P < .024$). SARS-CoV-2 and SARS-CoV were similar in cell tropism, with both targeting types I and II pneumocytes and alveolar macrophages. Importantly, despite the more efficient virus replication, SARS-CoV-2 did not significantly induce types I, II, or III interferons in the infected human lung tissues. In addition, while SARS-CoV infection upregulated the expression of 11 out of 13 (84.62%) representative proinflammatory cytokines/chemokines, SARS-CoV-2 infection only upregulated 5 of these 13 (38.46%) key inflammatory mediators despite replicating more efficiently.

Conclusions. Our study provides the first quantitative data on the comparative replication capacity and immune activation profile of SARS-CoV-2 and SARS-CoV infection in human lung tissues. Our results provide important insights into the pathogenesis, high transmissibility, and asymptomatic infection of SARS-CoV-2.

Keywords. coronavirus; COVID-19; ex vivo; interferon; SARS-CoV-2.

The novel coronavirus disease 2019 (COVID-19) pandemic caused by severe acute respiratory syndrome coronavirus 2 (SARS-CoV-2) has affected more than 2 000 000 patients with over 145 000 deaths within 4 months, whereas the 2002–2003 severe acute respiratory syndrome (SARS) caused by SARS-CoV was controlled within 6 months and only affected 8096 patients with 774 deaths [1, 2]. The genome of SARS-CoV-2 is most homologous to the Chinese horseshoe bat SARS-related coronaviruses and SARS-CoV-2 was speculated to have been transmitted from bats to a yet unknown wild animal being traded in a Wuhan wet market in China where this pandemic agent was first detected in the environmental samples [2, 3]. Apparently more efficient person-to-person transmission than 2003 SARS was soon noticed in the settings of families, churches, communities, cruise ships, nursing homes, and hospitals [4–8]. Despite the much lower crude fatality rate of COVID-19 (0.25–5%) than that of SARS (~10%), the high number of patients affected in this ongoing pandemic due to a complete lack of population herd immunity has resulted in a staggering number of deaths [9]. The clinical manifestations of COVID-19 can vary from asymptomatic virus shedding among household contacts, mild upper respiratory tract infection, and acute asymptomatic walking

Received 4 April 2020; editorial decision 6 April 2020; accepted 8 April 2020; published online April 9, 2020.

[a]Co–first authors.

Correspondence: K.-Y. Yuen, Department of Microbiology, Li Ka Shing Faculty of Medicine, State Key Laboratory of Emerging Infectious Diseases, Carol Yu Centre for Infection, Queen Mary Hospital, The University of Hong Kong, Room T19-026, Pokfulam, Hong Kong Special Administrative Region, China (kyyuen@hku.hk).

Clinical Infectious Diseases® 2020;71(6):1400–9

DOI: 10.1093/cid/ciaa410

pneumonia, to symptomatic pneumonia with bilateral multifocal ground-glass opacities on lung imaging studies and severe pneumonia with acute respiratory distress syndrome and multiorgan failure [10]. Although animal models of nonhuman primates, human angiotensin-converting enzyme 2 (ACE2) transgenic mice, and golden Syrian hamsters successfully challenged by SARS-CoV-2 have recently been reported, studies on the pathogenesis of COVID-19 in human subjects are still largely lacking [11–13]. While bronchoalveolar lavage was frequently performed in patients with severe COVID-19 to make a virologic diagnosis, transbronchial or open-lung biopsy for detecting the histopathological changes and host response in the human lung induced by SARS-CoV-2 was almost never performed to understand the pathogenesis in these patients with severe disease and respiratory failure. Postmortem examinations were also rarely performed until multiorgan failure developed after weeks of intensive care by intubation and ventilation [14]. In this study, we used ex vivo human lung tissue challenged by SARS-CoV-2 with SARS-CoV as a control to quantitatively characterize the viral kinetics, cell type tropism, virus protein expression, and host cytokine/chemokine responses. It is notable that the ex vivo lung tissue from each individual donor patient can be divided into 2 parts for a parallel challenge with SARS-CoV-2 and the control SARS-CoV. Thus, this ex vivo lung tissue organ culture model system provides a unique opportunity for side-by-side comparison of the virologic and host response characteristics that clinical studies on patients or animal models cannot achieve. The findings are important in understanding the relatively more efficient transmissibility of COVID-19 and the innate immune mechanism behind this phenomenon.

METHODS

Viruses and Biosafety

SARS-CoV-2 HKU-001a (GenBank accession number MT230904) was isolated from the nasopharyngeal aspirate of a patient with laboratory-confirmed COVID-19 in Hong Kong, as previously described [15]. SARS-CoV GZ50 (GenBank accession number AY304495) was an archived clinical isolate at the Department of Microbiology, The University of Hong Kong (HKU). Both SARS-CoV-2 and SARS-CoV were propagated and titered in VeroE6 cells with plaque assays, as previously described [15, 16]. All experiments involving infectious SARS-CoV-2 and SARS-CoV followed the approved standard operating procedures of our Biosafety Level 3 facility at the Department of Microbiology, HKU.

Human Ex Vivo Lung Tissues

Human lung tissues for ex vivo studies were obtained from patients undergoing surgical operations at Queen Mary Hospital, Hong Kong, as we previously described [17]. All donors gave written consent as approved by the Institutional Review Board of the University of Hong Kong/Hospital Authority Hong Kong West Cluster (UW13-364). The freshly obtained lung tissues were processed into small rectangular pieces and were rinsed with advanced Dulbecco's Modified Eagle's Medium (DMEM)/F12 medium (Gibco, Thermo Fisher Scientific) supplemented with 2 mM of 4-(2-hydroxyethyl)-1-piperazineethanesulfonic acid (HEPES) (Gibco), 1× GlutaMAX (Gibco), 100 U/mL penicillin, and 100 μg/mL streptomycin. The specimens were infected with SARS-CoV-2 or SARS-CoV with an inoculum of 1×10^6 plaque-forming units (PFU)/mL at 500 μL per well. After 2 hours, the inoculum was removed and the specimens were washed 3 times with phosphate-buffered saline (PBS). The infected human lung tissues were then cultured in 1.2 mL of advanced DMEM/F12 medium with 2 mM HEPES (Gibco), 1× GlutaMAX (Gibco), 100 U/mL penicillin, 100 μg/mL streptomycin, 20 μg/mL vancomycin, 20 μg/mL ciprofloxacin, 50 μg/mL amikacin, and 50 μg/mL nystatin. Supernatants were collected at 2, 24, and 48 hours postinoculation (hpi) for plaque assays. The lung tissues were harvested at 2, 24, and 48 hpi in RL buffer (Qiagen) with dithiothreitol (DTT) (Qiagen) for quantitative reverse transcription–polymerase chain reaction (qRT-PCR) analysis or fixed in 10% formalin for immunostaining and immunohistochemistry studies.

Immunofluorescence Staining and Confocal Microscopy

Immunofluorescence staining and confocal microscopy were performed as previously described with slight modifications [15, 18, 19]. Briefly, infected human lung tissue samples were harvested and fixed overnight using 10% formalin, and then processed with a TP1020 Leica semi-enclosed benchtop tissue processor with serially increasing concentrations of ethanol, xylene, and wax for 16 hours, before being embedded in wax. Formalin-fixed, paraffin-embedded human lung tissues were then sectioned at 4 μm with a Thermo Fisher Scientific HM 355S rotary microtome. Tissue sections were retrieved and dried to fix on Thermo Fisher Scientific Superfrost Plus slides at 37°C overnight before deparaffinizing and immunofluorescence staining. Serially increasing concentrations of xylene and ethanol were applied for dewaxing. In order to expose the viral nucleocapsid (N) antigens, the slides were heated with antigen unmasking solution (Vector Laboratories) in a pressure cooker for 90 seconds. After blocking with serum-free protein block and Sudan black B, the slides were stained with an in-house mouse anti–SARS-CoV-2-N immune serum or an in-house mouse anti–SARS-CoV-N immune serum. The secondary antibody goat anti-mouse immunoglobulin G (IgG) heavy and light chains (H&L) (Alexa Fluor 488) was obtained from Thermo Fisher Scientific. Mounting was performed with the antifade mounting medium with 4′,6-diamidino-2-phenylindole (DAPI) (Vector Laboratories). Images were acquired with confocal microscopy using a Zeiss LSM710 system with the 20× objective as previously described [20]. Image fields were selected and processed with the ZEN software blue edition (Zeiss) at a

resolution of 1024 × 1024 pixels. To quantify the relative fluorescence intensity, multiple images from infected human lung tissues of 2 representative donors were split into separate channels and the intensity of channel 488 nm was quantified with ImageJ software (National Institutes of Health).

Histology and Immunohistochemical Staining

Histology and immunohistochemical staining was performed as previously described with slight modifications [13]. Briefly, fixed human tissues were processed, embedded, and cut to prepare 4-μm tissue sections on glass slides. Slides were dewaxed with xylene and serially decreased concentrations of ethanol before staining. To detect SARS-CoV-2-N and SARS-CoV-N antigens, tissue sections underwent the same antigen retrieval procedures as those of immunofluorescence staining, followed by blocking with 0.3% hydrogen peroxide for 30 minutes to abolish the activity of any potential endogenous peroxidase. The slides were subsequently incubated with an in-house mouse anti–SARS-CoV-2-N immune serum or an in-house mouse anti–SARS-CoV-N immune serum, and then incubated with Mouse-on-Mouse Polymer (Abcam). The signal was developed with the DAB (3,3′-diaminobenzidine) substrate kit (Vector Laboratories). The nuclei were developed with Gill's hematoxylin before mounting the slides with VectaMount permanent mounting medium (Vector Laboratories). Images were acquired with the Olympus BX53 light microscope using a 40× objective.

Plaque Assays

VeroE6 cells were maintained in DMEM with 10% FBS, 1% penicillin, and 1% streptomycin. The cells were seeded 1 day before the experiment at 2×10^5 cells per well in 12-well plates and were allowed to grow at 37°C overnight. For the plaque assay, serially diluted samples were inoculated on the cells for 1 hour. Afterwards, 3% agarose/PBS was mixed with DMEM with 1.5% fetal bovine serum at a 1:2 ratio and applied to the cells. The cells were incubated for 96 hours for plaque formation. The plaques were visualized by staining the plates with 1% crystal violet in 20% ethanol/distilled water for 15 minutes.

RNA Extraction and Quantitative Reverse Transcription–Polymerase Chain Reaction

Cell lysate samples from the infected lung tissues were harvested at 2, 24, and 48 hpi for qRT-PCR detection of mRNA levels of interferon (IFN) and cytokine/chemokine markers. Briefly, lung tissues were homogenized and lysed with RL buffer for RNA extraction using the RNeasy Mini kit (Qiagen). Quantitative reverse transcription–polymerase chain reaction was then performed using the QuantiNova SYBR Green RT-PCR kit (Qiagen) with the LightCycler 480 Real-Time PCR System (Roche) to quantify the expression level of different host markers. Each 20-μL reaction mixture contained 10 μL of 2× QuantiNova SYBR Green RT PCR Master Mix, 2.6 μL of RNase-free water, 0.2 μL of QuantiNova SYBR Green RT-Mix, 1.6 μL each of 10 μM gene-specific forward and reverse primer, and 4 μL of extracted RNA as template. Reactions were incubated at 45°C for 10 minutes for reverse transcription, 95°C for 5 minutes for denaturation, followed by 45 cycles of 95°C for 5 seconds and 55°C for 30 seconds. Signal detection and measurements were taken in each cycle after the annealing step. The cycling profile ended with a cooling step at 40°C for 30 seconds. The primer sequences are available upon request.

Statistical Analysis

Statistical analyses for the quantification of viral N antigen expression from SARS-CoV-2– or SARS-CoV–infected human lung tissues were performed with 1-way ANOVA using GraphPad Prism 6 (GraphPad Software, Inc). Statistical analyses for the area under the curve (AUC) comparison between SARS-CoV-2– and SARS-CoV–generated infectious virus particles from the infected human lung tissues were performed with Student's *t* test using GraphPad Prism 6 as previously described [15]. Statistical analyses for SARS-CoV-2– or SARS-CoV–induced cytokine/chemokine expressions were performed with 2-way ANOVA using GraphPad Prism 6. Differences were considered statistically significant when $P < .05$.

RESULTS

Comparative Infection and Replication Capacity of SARS-CoV-2 and SARS-CoV in Ex Vivo Human Lung Tissue Explants

A total of 6 patient donors were included in this study. These included 3 females and 3 males with a mean age of 53 years (range, 47–64 years) who underwent wedge resection or lobectomy for lung tumor. To evaluate their differential capacities to infect and replicate in human lung tissue, we inoculated human lung tissue explants with SARS-CoV-2 or SARS-CoV with an inoculum of 1×10^6 PFU/mL at 500 μL per well. The infected samples were harvested at 24 hpi and examined for viral N antigen expression. With immunostaining and confocal microscopy, we demonstrated that both SARS-CoV-2 and SARS-CoV could infect human lung tissues as evidenced by viral N antigen expression in representative images of 2 donors (Figure 1). Intriguingly, SARS-CoV-2-N antigens were consistently detected in higher abundance and in broader areas of the lung tissues of all donors than SARS-CoV-N antigens (Figure 1). Quantitative analysis confirmed that the relative fluorescent intensity of SARS-CoV-2-N antigen was significantly ($P < .0001$ to .041) higher (2.30- to 2.87-fold) than SARS-CoV-N antigen in the donors' lung tissues (Supplementary Figure 1). To more thoroughly quantify the different infectiveness and replication of the 2 viruses in human lung tissues, we inoculated additional lung tissue samples and measured the infectious virus titers generated at 2, 24, and 48 hpi with plaque assays. Among the 4 lung tissues evaluated, the maximum SARS-CoV-2 titer increased between 2 hpi and 48 hpi and ranged from 1.20-log to 2.04-log. With the same experimental

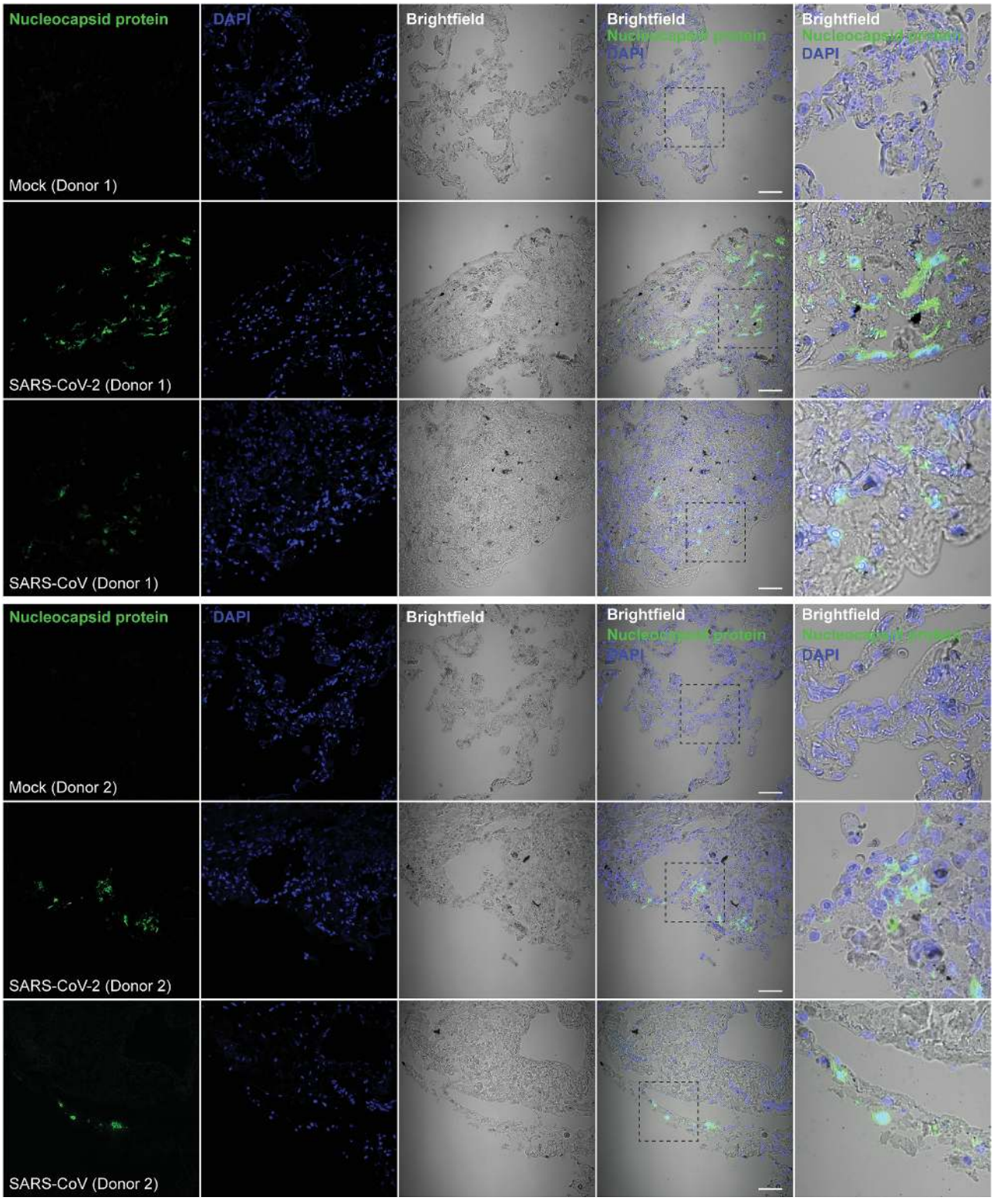

Figure 1. Confocal microscopy examination of SARS-CoV-2 and SARS-CoV replication in human lung tissues. Human lung tissues were challenged with SARS-CoV-2 or SARS-CoV with an inoculum of 1×10^6 PFU/mL. At 24 hpi, the infected lung tissues were harvested, fixed in 10% formalin, and immunolabeled for viral antigen. SARS-CoV-2-nucleocapsid (N) antigens were identified with an in-house mouse anti–SARS-CoV-2-N immune serum, and SARS-CoV-N antigens were identified with an in-house mouse anti–SARS-CoV-N immune serum. Representative images from 2 lung donors are shown. The experiment was repeated with another 4 donors with consistent findings. Bars represent 50 μm. Dotted square, areas to be enlarged and shown in the insets. Abbreviations: hpi, hours postinoculation; PFU, plaque-forming units; SARS-CoV, severe acute respiratory syndrome coronavirus; SARS-CoV-2, severe acute respiratory syndrome coronavirus 2.

setting, the maximum SARS-CoV titer increase between 2 hpi and 48 hpi ranged from 0.61-log to 1.15-log only (Figure 2A). To determine the relative replication capacity of the 2 viruses in lung tissues, we set the virus titer at 2 hpi as the baseline, which represented the residual inoculum after inoculation and wash, and calculated the virus titer increase from the baseline at 24 and 48 hpi. As shown in Figure 2B, SARS-CoV-2 consistently demonstrated higher virus titer increases than did SARS-CoV in lung tissues from all 4 donors. Our AUC analysis revealed that SARS-CoV-2 generated 3.20-fold more infectious virus particles than did SARS-CoV from the infected lung tissues over a period of 48 hours ($P < .024$) (Figure 2C). Taken together, our results illustrate that SARS-CoV-2 was capable of infecting and replicating more robustly than SARS-CoV in human lung tissues.

Cell Tropism of SARS-CoV-2 and SARS-CoV in Human Lung Tissues

To identify the cell types targeted by SARS-CoV-2 and SARS-CoV in the human lung, we performed immunohistochemical staining

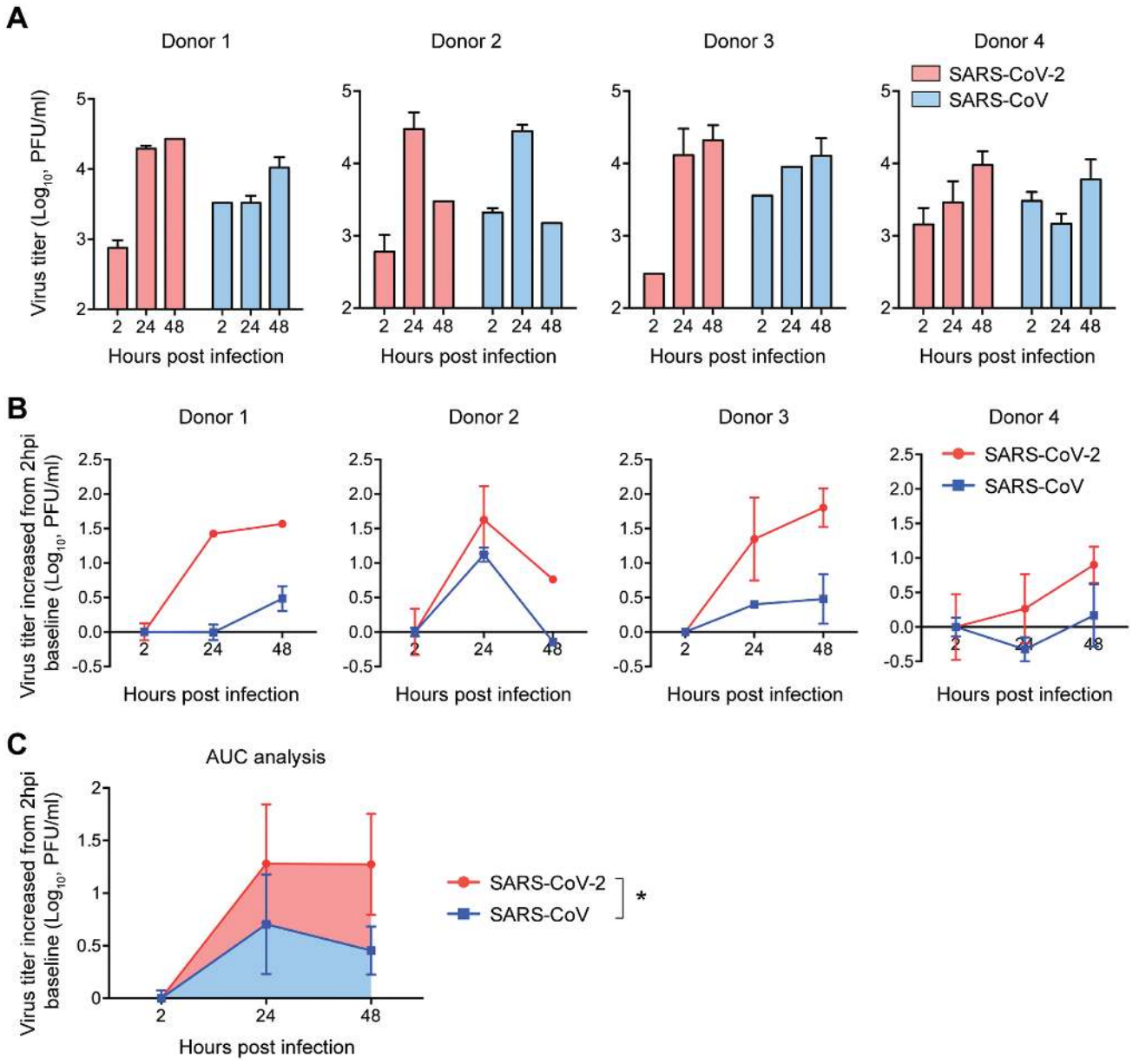

Figure 2. Comparative replication capacity of SARS-CoV-2 and SARS-CoV in human lung tissues. Human lung tissues from 4 independent donors were challenged with SARS-CoV-2 or SARS-CoV. Supernatant samples from the infected lung tissues were harvested at 2, 24, and 48 hpi. The virus titers were determined with plaque assays. *A*, The virus titers of the 4 individual lung tissues. *B*, The amount of infectious virus particles increased over the 48-hour period upon SARS-CoV-2 or SARS-CoV inoculation for each lung donor. *C*, AUC analysis of SARS-CoV-2– and SARS-CoV–infected human lung tissues, demonstrating the total amount of live infectious virus particles generated over the 48-hour period. Results in panel *C* represent the means and SDs from 4 independent donors from 4 independent experiments. Statistical significance in panel *C* was determined with Student *t* test. **P* < .05. Abbreviations: AUC, area under the curve; hpi, hours postinfection; SARS-CoV, severe acute respiratory syndrome coronavirus; SARS-CoV-2, severe acute respiratory syndrome coronavirus 2.

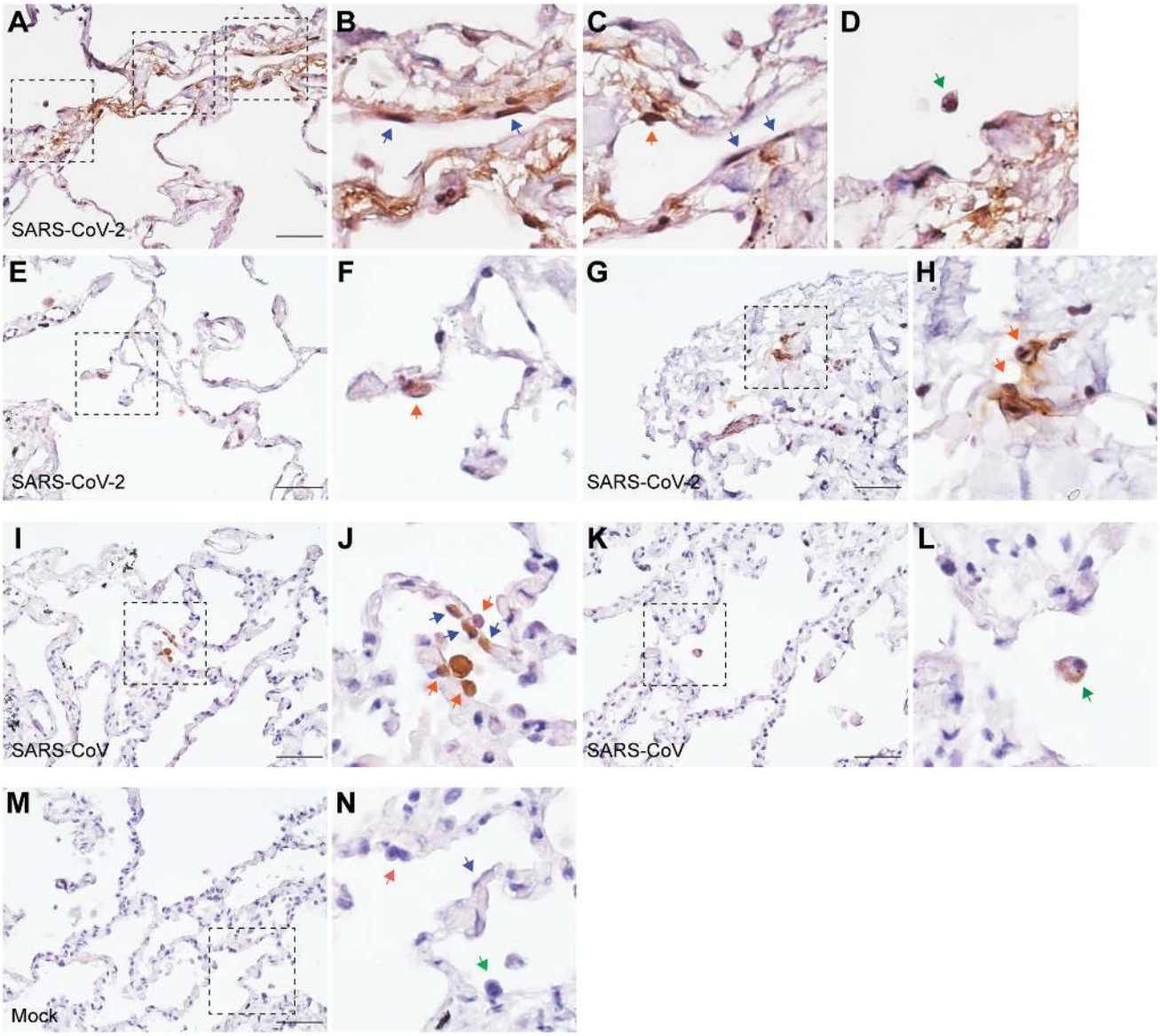

Figure 3. Cell tropism of SARS-CoV-2 and SARS-CoV in human lung tissues. Human lung tissues were challenged with SARS-CoV-2 or SARS-CoV. At 24 hpi, the infected lung tissues were harvested, fixed in 10% formalin, and processed for immunohistochemical examination of viral antigen. *A–H*, SARS-CoV-2-nucleocapsid (N) antigens could be identified from type I pneumocytes (*B, C*), type II pneumocytes (*C, F, H*), and alveolar macrophages (*D*). *I–L*, SARS-CoV-N antigens could be identified from type I pneumocytes and type II pneumocytes (*J*), as well as alveolar macrophages (*L*). *M* and *N*, Mock-infected human lung tissues processed and immunolabeled with the same set of antibodies did not show any specific signal. SARS-CoV-2-N antigens were identified with an in-house mouse anti–SARS-CoV-2-N immune serum, and SARS-CoV-N antigens was identified with an in-house mouse anti–SARS-CoV-N immune serum. Blue arrows represent type I pneumocytes, orange arrows represent type II pneumocytes, and green arrows represent alveolar macrophages. The experiment was repeated with 3 donors with consistent findings. Bars represent 50 μm. Dotted square, areas to be enlarged and shown in the insets. Abbreviations: hpi, hours postinoculation; SARS-CoV, severe acute respiratory syndrome coronavirus; SARS-CoV-2, severe acute respiratory syndrome coronavirus 2.

of the virus-infected lung tissues (Figure 3). Our results clearly demonstrated that SARS-CoV-2 could infect type I pneumocytes (Figure 3A–C), type II pneumocytes (Figure 3E–H), as well as alveolar macrophages (Figure 3D). In this regard, the cell tropism of SARS-CoV-2 in the human lung was similar to that of SARS-CoV, which also targeted types I and II pneumocytes (Figure 3I, J) and alveolar macrophages (Figure 3K, L). Viral N antigen signal was not detected from mock-infected samples (Figure 3M, N).

Expression Profiles of Interferons and Proinflammatory Mediators in SARS-CoV-2– and SARS-CoV–Infected Human Lung Tissues

Next, to assess the innate immune responses induced by SARS-CoV-2 and SARS-CoV in human lung tissues, we investigated the expression of a panel of representative IFNs and proinflammatory cytokines/chemokines upon virus challenge. Our data demonstrated that the 2003 SARS-CoV infection resulted in significant upregulation of types I (IFNβ), II (IFNγ), and III (IFNλ1, IFNλ2, and IFNλ3) IFNs

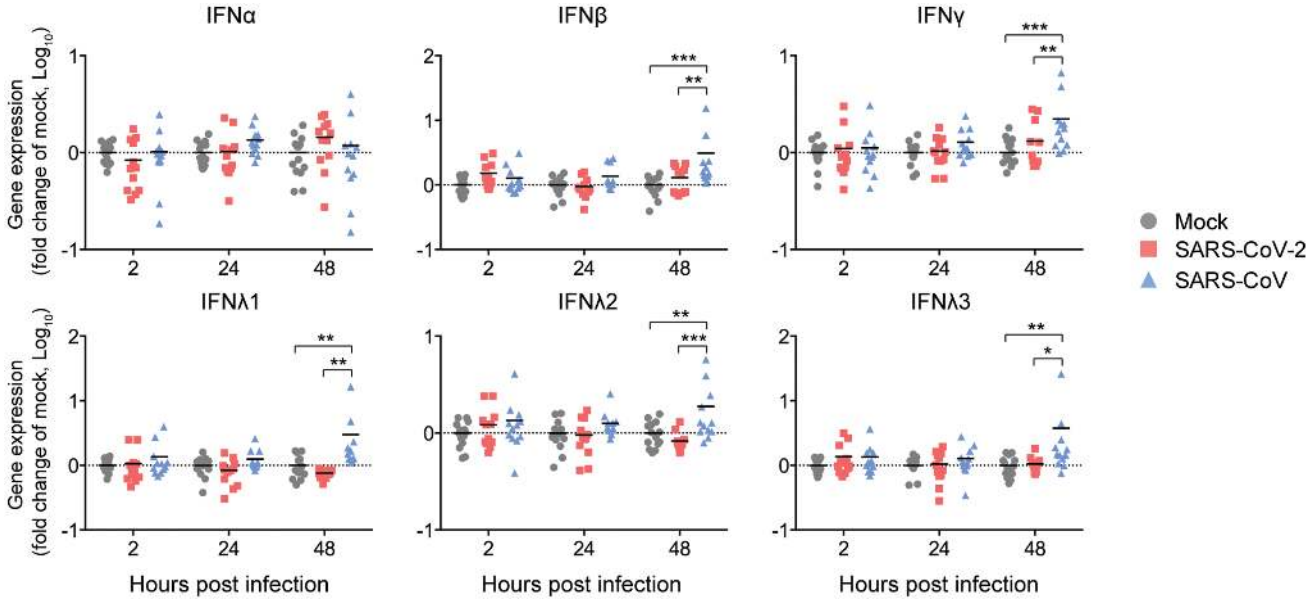

Figure 4. Interferon response of SARS-CoV-2– and SARS-CoV–infected human lung tissues. Human lung tissues were challenged with SARS-CoV-2 or SARS-CoV. At 2, 24, and 48 hpi, the infected lung tissues were harvested for qRT-PCR analysis of type I (IFNα and IFNβ), type II (IFNγ), and type III (IFNλ1, IFNλ2, and IFNλ3) interferons. The results represent values from 4 independent lung donors in 4 independent experiments, with 3–5 lung samples per donor. Statistical significance was determined with 2-way ANOVA. $^{*}P < .05$, $^{**}P < .01$, $^{***}P < .001$. Abbreviations: ANOVA, analysis of variance; hpi, hours postinfection; qRT-PCR, quantitative reverse transcription–polymerase chain reaction; SARS-CoV, severe acute respiratory syndrome coronavirus; SARS-CoV-2, severe acute respiratory syndrome coronavirus 2.

in human lung tissues. In contrast, SARS-CoV-2 infection did not significantly trigger the expression of any IFN at all evaluated time points (Figure 4). In addition to types I, II, and III IFNs, we evaluated the expression of 4 key proinflammatory cytokines (Figure 5A) and 9 key proinflammatory chemokines (Figure 5B) that have critical roles in immune cell recruitment and activation. Our data show that SARS-CoV infection resulted in significant activation of 11 out of 13 (84.62%) evaluated proinflammatory factors at either 24 hpi or 48 hpi. In contrast, SARS-CoV-2 infection only significantly upregulated 5 of these 13 (38.46%) inflammatory mediators including interleukin-6 (IL6), monocyte chemoattractant protein-1 (MCP-1), chemokine (C-X-C motif) ligand 1 (CXCL1), chemokine (C-X-C motif) ligand 5 (CXCL5), and chemokine (C-X-C motif) ligand 10 (CXCL10/IP10). In addition, among all assessed IFNs and cytokines/chemokines, the expression of 12 out of 19 (63.16%) genes were significantly lower in SARS-CoV-2–infected human lung tissues in comparison to that of the SARS-CoV–infected samples (Figures 4 and 5). Only IP10 was significantly more induced by SARS-CoV-2 than SARS-CoV. Collectively, our results illustrate that SARS-CoV-2 generally triggered significantly lower levels of IFNs and proinflammatory cytokines/chemokines despite being capable of infecting and replicating in the human lung at a significantly higher efficiency.

DISCUSSION

Using ex vivo human lung tissue explants respectively challenged by the same inoculum of SARS-CoV-2 and SARS-CoV, we showed that SARS-CoV-2 was more capable than SARS-CoV of infecting and replicating in human lung tissues. While both viruses infected type I and type II pneumocytes, and alveolar macrophages as target cells, the amount of viral N antigen expression in the virus-challenged lung tissues was significantly higher and more intensive in the tissues infected with SARS-CoV-2 than in those infected with SARS-CoV. Moreover, SARS-CoV-2 produced 3.20-fold higher amounts of infectious virus particles than did SARS-CoV within 48 hpi. These findings might explain the high viral load in the respiratory secretions of patients with COVID-19 during the early days after presentation or even during incubation, and thus its high person-to-person transmissibility [4, 21]. Importantly, we demonstrated that SARS-CoV-2 triggered lower levels of IFNs and proinflammatory cytokines/chemokines despite being capable of infecting and producing significantly higher amount of virus in human lung tissues. While the innate immune response in infected cells is our first line of defense against acute viral infection, SARS-CoV-2 infection did not significantly trigger any IFN response at all, and only significantly activated 5 of 13 proinflammatory mediators. Thus, unlike patients with SARS who generally presented with high fever followed by rapidly progressive pneumonia and then respiratory failure with a mortality rate of approximately 10%, only approximately 16% of patients with COVID-19 are severely ill and less than 5% of them died [2, 10]. The low degree of innate immune activation could also account for the mild or even lack of symptoms in many patients with COVID-19 who were not even tested and unknowingly spreading the virus in both community and hospital settings, making the control of the pandemic much more difficult than SARS.

While both 2019 SARS-CoV-2 and 2003 SARS-CoV can attach and enter host cells via ACE2, the mechanism of how

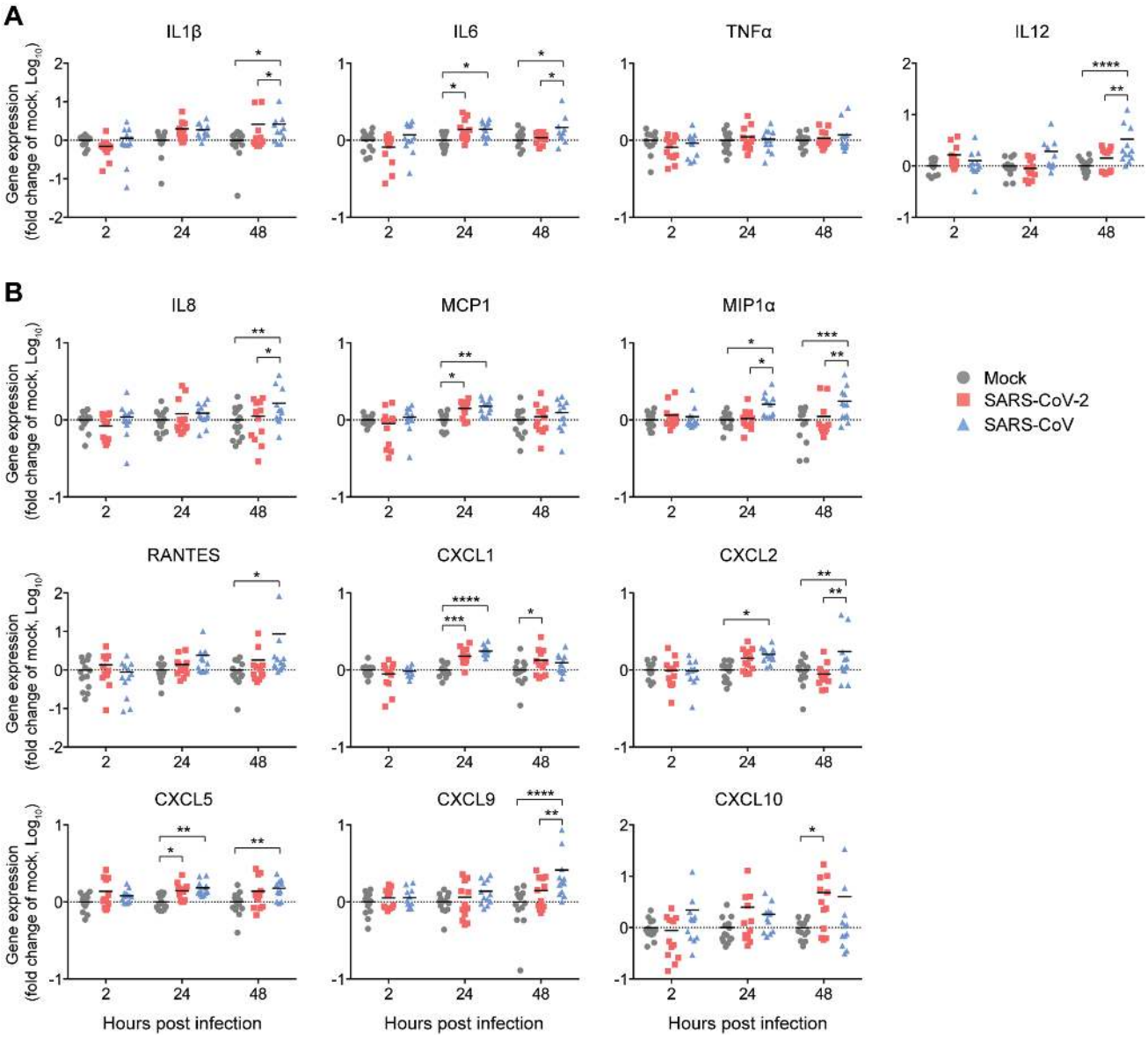

Figure 5. Expression profile of proinflammatory cytokines and chemokines from SARS-CoV-2– and SARS-CoV–infected human lung tissues. Human lung tissues were challenged with SARS-CoV-2 or SARS-CoV. At 2, 24, and 48 hpi, the infected lung tissues were harvested for qRT-PCR analysis of representative proinflammatory cytokines (*A*) and chemokines (*B*). The results represent values from 4 independent lung donors in 4 independent experiments, with 3–5 lung samples per donor. Statistical significance was determined with 2-way ANOVA. $^{*}P < .05$, $^{**}P < .01$, $^{***}P < .001$, $^{****}P < .0001$. Abbreviations: ANOVA, analysis of variance; CXCL1, chemokine (C-X-C motif) ligand 1; CXCL10, chemokine (C-X-C motif) ligand 10; CXCL2, chemokine (C-X-C motif) ligand 2; CXCL5, chemokine (C-X-C motif) ligand 5; CXCL9, chemokine (C-X-C motif) ligand 9; hpi, hours postinoculation; IL, interleukin; IL12, interleukin 12; IL1β, interleukin 1 beta; IL6, interleukin 6; IL8, interleukin 8; MCP1, monocyte chemoattractant protein 1; MIP1α, macrophage inflammatory protein 1 alpha; qRT-PCR, quantitative reverse transcription–polymerase chain reaction; RANTES, regulated on activation, normal T cell expressed and secreted; SARS-CoV, severe acute respiratory syndrome coronavirus; SARS-CoV-2, severe acute respiratory syndrome coronavirus 2; TNFα, tumor necrosis factor α.

SARS-CoV-2 overcomes the innate immune response and suppresses the IFN and proinflammatory cytokines and chemokines to achieve a higher degree of viral replication is still elusive. Although the N protein of both of these coronaviruses share 94% of amino acid similarity [3], significantly higher N expression in terms of both the extent and intensity was readily observed in SARS-CoV-2–infected ex vivo lung tissues. Studies of SARS-CoV in cell culture suggested that its N protein antagonized IFNβ response in a dose-dependent manner [22]. Moreover, 2 other SARS-CoV proteins, namely open reading frame (Orf) 3b and Orf6, also antagonize IFN synthesis and signaling [23]. While SARS-CoV-2 is also postulated to possess IFN-antagonizing proteins, the exact identities of these proteins remain undetermined at this stage. The differential degrees of IFN inhibition by these viruses' IFN-antagonizing proteins may explain the discrepant viral replications and inflammatory responses in human lungs

observed in the present study. Moreover, most proinflammatory cytokines and chemokines except for IP10, a chemoattractant for monocytes/macrophages, T cells, and natural killer (NK) cells, were more significantly induced by SARS-CoV than SARS-CoV-2. This finding may explain the more severe disease and higher mortality of SARS than of COVID-19.

In contrast to patients with SARS who had increasing viral load in nasopharyngeal secretions that peaked at approximately day 10, the viral load in the respiratory secretions of patients with COVID-19 peaked much earlier at the time of symptom onset [21, 24]. The viral kinetics and innate immune response profiles in ex vivo human lung tissue characterized in this study might help to explain this observation. The suboptimally activated innate immune response would allow SARS-CoV-2 to replicate to high levels in the respiratory tract early on and may contribute to its efficient person-to-person transmission via droplets or contact with contaminated respiratory secretions containing high viral loads [4, 21, 25]. Notably, the higher degree of viral infection and replication of SARS-CoV-2 in human lung tissues corroborated our recent finding that SARS-CoV-2 exhibited more efficient replication in Calu3 (human lung adenocarcinoma) cells than SARS-CoV [15].

Our findings have important implications for the infection-control and treatment strategies for COVID-19 as patients with SARS-CoV-2 may be infectious during the incubation period before onset of clinical symptoms due to its efficient modulation of host innate immune and proinflammatory response, as evidenced by our findings [26]. Thus, in addition to hand washing and social distancing, universal masking was recommended in East Asia as a key epidemiological control measure to prevent virus shedding from subclinical patient sources and to prevent infection of susceptible individuals in the community [27]. Similar to influenza, which is the most well-studied acute respiratory virus infection, the viral load in the respiratory secretions of patients with COVID-19 also peaks at the time of symptom onset, and antiviral treatment for COVID-19 may be less effective if given later than 48 hours after symptom onset. Thus, unlike SARS and Middle East respiratory syndrome which have viral loads peaking at day 7 to day 10 and therefore sufficient time for antivirals to act and reduce the peak viral loads, early initiation of antiviral therapy would be even more important to improve the clinical outcome of COVID-19 [24, 28]. Moreover, the use of high-dose corticosteroids and antagonists against major inflammatory mediators such as IL6 should only be used together with effective antivirals to avoid oversuppression of the innate immune response in patients with COVID-19 as SARS-CoV-2 is already modulating the host innate immune response at the beginning of the infection [29].

There are limitations to this study. First, the ex vivo human lung tissue explant culture is short-lasting and cannot represent the effect of host systemic inflammatory response and the adaptive immune response. Second, the supply of human lung tissues is limited and thus it was not possible for us to investigate the characteristics of different SARS-CoV-2 strains in this ex vivo model. More studies should be performed using both ex vivo lung and intestinal organoids to elucidate additional details on the pathogenesis of SARS-CoV-2 during pulmonary and extrapulmonary involvement.

Supplementary Data

Supplementary materials are available at *Clinical Infectious Diseases* online. Consisting of data provided by the authors to benefit the reader, the posted materials are not copyedited and are the sole responsibility of the authors, so questions or comments should be addressed to the corresponding author.

Notes

Author contributions. H. C., J. F.-W. C., and K.-Y. Y. had roles in the study design, data collection, data analysis, data interpretation, and writing of the manuscript. Y. W., T. T.-T. Y, Y. C., Y. H., H. S., D. Y., B. H., X. H., X. Z., J.-P. C., J. Z., S. Y., K.-H. K., K. K.-W. T., I. H.-Y. C., A. J. Z., K.-Y. S., and W.-K. A. had roles in the experiments, data collection, data analysis, and data interpretation. All authors reviewed and approved the final version of the manuscript.

Disclaimer. The funding sources had no role in the study design, data collection, analysis, interpretation, or writing of the report

Financial support. This study was partly supported by the donations of May Tam Mak Mei Yin, Richard Yu, and Carol Yu, the Shaw Foundation Hong Kong; Michael Seak-Kan Tong, Respiratory Viral Research Foundation Limited; Hui Ming, Hui Hoy and Chow Sin Lan Charity Fund Limited; Chan Yin Chuen Memorial Charitable Foundation; Marina Man-Wai Lee, the Hong Kong Hainan Commercial Association South China Microbiology Research Fund; the Jessie & George Ho Charitable Foundation, and Perfect Shape Medical Limited and received funding from the Consultancy Service for Enhancing Laboratory Surveillance of Emerging Infectious Diseases and Research Capability on Antimicrobial Resistance for Department of Health of the Hong Kong Special Administrative Region Government; the Theme-Based Research Scheme (grant number T11/707/15) of the Research Grants Council; Hong Kong Special Administrative Region; Sanming Project of Medicine in Shenzhen, China (grant number SZSM201911014); and the High Level-Hospital Program, Health Commission of Guangdong Province, China.

Potential conflicts of interest. The authors: No reported conflicts of interest. All authors have submitted the ICMJE Form for Disclosure of Potential Conflicts of Interest.

References

1. Cheng VC, Lau SK, Woo PC, Yuen KY. Severe acute respiratory syndrome Coronavirus as an agent of emerging and reemerging infection. Clin Microbiol Rev **2007**; 20:660–94.
2. World Health Organization. Coronavirus disease (COVID-19) situation report—74. 3 April 2020. Available at: https://www.who.int/docs/default-source/coronaviruse/situation-reports/20200403-sitrep-74-covid-19-mp.pdf?sfvrsn=4e043d03_4. Accessed 4 April 2020.
3. Chan JF, Kok KH, Zhu Z, et al. Genomic characterization of the 2019 novel human-pathogenic coronavirus isolated from a patient with atypical pneumonia after visiting Wuhan. Emerg Microbes Infect **2020**; 9:221–36.
4. Chan JF, Yuan S, Kok KH, et al. A familial cluster of pneumonia associated with the 2019 novel coronavirus indicating person-to-person transmission: a study of a family cluster. Lancet **2020**; 395:514–523. doi:10.1016/S0140-6736(20)30154-9
5. Cheng VCC, Wong SC, Chen JHK, et al. Escalating infection control response to the rapidly evolving epidemiology of the coronavirus disease 2019 (COVID-19) due to SARS-CoV-2 in Hong Kong. Infect Control Hosp Epidemiol **2020**; 1–6. Epub ahead of print. doi:10.1017/ice.2020.58
6. Rocklov J, Sjodin H, Wilder-Smith A. COVID-19 outbreak on the Diamond Princess cruise ship: estimating the epidemic potential and effectiveness of public health countermeasures. J Travel Med **2020;** pii:taaa030. Epub ahead of print. doi: 10.1093/jtm/taaa030
7. McMichael TM, Currie DW, Clark S, et al. Epidemiology of Covid-19 in a long-term care facility in King County, Washington. N Engl J Med **2020**. Epub ahead of print. doi:10.1056/NEJMoa2005412

8. Pung R, Chiew CJ, Young BE, et al; Singapore 2019 Novel Coronavirus Outbreak Research Team. Investigation of three clusters of COVID-19 in Singapore: implications for surveillance and response measures. Lancet **2020**; 395:1039–46.
9. Wilson N, Kvalsvig A, Barnard LT, Baker MG. Case-fatality risk estimates for COVID-19 calculated by using a lag time for fatality. Emerg Infect Dis **2020**; 26. Epub ahead of print. doi:10.3201/eid2606.200320
10. Guan WJ, Ni ZY, Hu Y, et al. Clinical characteristics of coronavirus disease 2019 in China. N Engl J Med **2020**. Epub ahead of print. doi:10.1056/NEJMoa2002032
11. Bao L, Deng W, Gao H, et al. Reinfection could not occur in SARS-CoV-2 infected rhesus macaques. **2020**. Available at: https://www.biorxiv.org/content/10.1101/2020.03.13.990226v1. Accessed 3 April 2020.
12. Bao L, Deng W, Huang B, et al. The pathogenicity of SARS-CoV-2 in hACE2 transgenic mice. **2020**. Available at: https://www.biorxiv.org/content/10.1101/2020.02.07.939389v3. Accessed 3 April 2020.
13. Chan JF, Zhang AJ, Yuan S, et al. Simulation of the clinical and pathological manifestations of coronavirus disease 2019 (COVID-19) in golden Syrian hamster model: implications for disease pathogenesis and transmissibility. Clin Infect Dis **2020**. pii:ciaa325. Epub ahead of print. doi:10.1093/cid/ciaa325
14. Tian S, Hu W, Niu L, Liu H, Xu H, Xiao SY. Pulmonary pathology of early-phase 2019 novel coronavirus (COVID-19) pneumonia in two patients with lung cancer. J Thorac Oncol **2020.** pii:S1556-0864(20)30132-5. Epub ahead of print. doi:10.1016/j.jtho.2020.02.010
15. Chu H, Chan JF, Yuen TT, et al. Comparative tropism, replication kinetics, and cell damage profiling of SARS-CoV-2 and SARS-CoV with implications for clinical manifestations, transmissibility, and laboratory studies of COVID-19: an observational study. Lancet Microbe **2020**. doi:10.1016/S2666-5247(20)30004-5
16. Chan JF, Yip CC, To KK, et al. Improved molecular diagnosis of COVID-19 by the novel, highly sensitive and specific COVID-19-RdRp/Hel real-time reverse transcription-polymerase chain reaction assay validated in vitro and with clinical specimens. J Clin Microbiol **2020**. pii:JCM.00310-20. Epub ahead of print. doi:10.1128/JCM.00310-20
17. Zhou J, Chu H, Li C, et al. Active replication of Middle East respiratory syndrome coronavirus and aberrant induction of inflammatory cytokines and chemokines in human macrophages: implications for pathogenesis. J Infect Dis **2014**; 209:1331–42.
18. Chu H, Chan CM, Zhang X, et al. Middle East respiratory syndrome coronavirus and bat coronavirus HKU9 both can utilize GRP78 for attachment onto host cells. J Biol Chem **2018**; 293:11709–26.
19. Chan CM, Chu H, Wang Y, et al. Carcinoembryonic antigen-related cell adhesion molecule 5 is an important surface attachment factor that facilitates entry of Middle East respiratory syndrome coronavirus. J Virol **2016**; 90:9114–27.
20. Chu H, Zhou J, Wong BH, et al. Middle East respiratory syndrome coronavirus efficiently infects human primary T lymphocytes and activates the extrinsic and intrinsic apoptosis pathways. J Infect Dis **2016**; 213:904–14.
21. To KK, Tsang OT, Leung WS, et al. Temporal profiles of viral load in posterior oropharyngeal saliva samples and serum antibody responses during infection by SARS-CoV-2: an observational cohort study. Lancet Infect Dis **2020**.
22. Hu Y, Li W, Gao T, et al. The severe acute respiratory syndrome coronavirus nucleocapsid inhibits type I interferon production by interfering with TRIM25-mediated RIG-I ubiquitination. J Virol **2017**; 91.
23. Kopecky-Bromberg SA, Martínez-Sobrido L, Frieman M, Baric RA, Palese P. Severe acute respiratory syndrome coronavirus open reading frame (ORF) 3b, ORF 6, and nucleocapsid proteins function as interferon antagonists. J Virol **2007**; 81:548–57.
24. Peiris JS, Chu CM, Cheng VC, et al; HKU/UCH SARS Study Group. Clinical progression and viral load in a community outbreak of coronavirus-associated SARS pneumonia: a prospective study. Lancet **2003**; 361:1767–72.
25. To KK, Tsang OT, Chik-Yan Yip C, et al. Consistent detection of 2019 novel coronavirus in saliva. Clin Infect Dis **2020**.
26. Wei WE, Li Z, Chiew CJ, et al. Presymptomatic transmission of SARS-CoV-2—Singapore, January 23–March 16, 2020. MMWR Morb Mortal Wkly Rep **2020** [Epub ahead of print] doi: 10.15585/mmwr.mm6914e1.
27. Chan KH, Yuen KY. COVID-19 epidemic: disentangling the re-emerging controversy about medical facemasks from an epidemiological perspective. Int J Epidemiol **2020**; pii:dyaa044.
28. Chan JF, Lau SK, To KK, Cheng VC, Woo PC, Yuen KY. Middle East respiratory syndrome coronavirus: another zoonotic betacoronavirus causing SARS-like disease. Clin Microbiol Rev **2015**; 28:465–522.
29. Xu X, Han M, Li T, et al. Effective treatment of severe COVID-19 patients with Tocilizumab. Available at: http://chinaxiv.org/home.htm ChinaXiv 2020. Accessed 3 April 2020.